Collective coordinates in one-dimensional soliton models revisited

I. Takyi and H. Weigel

Physics Department, Stellenbosch University, Matieland 7602, South Africa

We compare numerical solutions to the full field equations to simplified approaches based on implementing three collective coordinates for kink-antikink interactions within the φ^4 and ϕ^6 models in one time and one space dimensions. We particularly pursue the question whether the collective coordinate approximation substantiates the conjecture that vibrational modes are important for resonance structures to occur in kink-antikink scattering.

I. INTRODUCTION

The φ^4 model is a nonlinear prototype extension of the Klein-Gordon theory in one time and one space dimensions which contains soliton solutions (more precisely solitary waves) [1] that possess localized energy densities. Nonlinearity gives rise to distinct vacuum solutions and the solitons connect different vacua at negative and positive spatial infinity. These solitons are called kinks and have a particlelike behavior when subjected to external forces. Configurations obtained by spatial reflection are antikinks. Similar soliton solutions are found in the sine-Gordon and ϕ^6 models. Nonintegrability of the φ^4 and ϕ^6 models makes them more interesting because of the enriched structure of solutions that correspond to kink-antikink interactions. Localized soliton-type solutions are not limited to these models. For example, lumplike configurations were obtained in modified φ^4 models [2] and kink-kink solutions in models with nonpolynomial potentials [3]. Solitons in the ϕ^8 model have been recently constructed in Ref. [4].

There is a wide range of applications for (anti)kink solutions in physics: In cosmology [5,6] the kink solutions describe the fractal structure of domain walls [7]; in condensed matter physics they mimic domain walls in ferromagnets [8] and ferroelectrics [9]. A remarkable feature of solitons is that their (classical) energy is inversely proportional to the coupling constant. Considering the number of colors in quantum chromodynamics as a hidden coupling constant [10] thus motivates us to regard baryons as solitons in an effective meson theory [11]. This picture of baryons has proven quite successful in describing many baryon properties [12]. This approach has even been generalized to nuclei [13]. A general discussion of (topological) solitons can be obtained from Ref. [14].

Besides the zero mode associated with spontaneous breaking of translational invariance, the fluctuation spectrum about the φ^4 kink contains a further bound state, the so-called shape mode. This shape mode possesses a number of interesting features. For example, it can be indirectly excited by external forces [15] and the frequency of wobbling kinks is correlated with the bound state energy

of the shape mode [16]. On the other hand the numerically observed frequencies of oscillons (long-living oscillations generated from an initial bump) are lower than the eigenfrequency of the shape mode [17]. This mode is a bound state in the background of the (anti)kink and thus represents an essential vibrational excitation of the (anti) kink. In kink-antikink scattering this mode might temporarily store energy and release it at a later time [18]. This process has been considered to be responsible for resonance phenomena in this scattering reaction: with energy stored in the shape mode, kinks and antikinks do not have enough energy to fully separate. Remarkably, such resonance solutions have also been observed in the ϕ^6 model [19]. However, this model does not contain the shape mode. Of course, the interplay of translational and vibrational modes during the kink-antikink interaction is an interesting subject on its own that has been generalized to multiple kink interactions recently [20].

The above survey is certainly incomplete but sufficient to demonstrate that there is a rich structure[1] of solitons in nonlinear low-dimensional models that can be identified by numerical simulations which are not too laborious. It is interesting and challenging to identify the dynamics behind these structures. A technique that has been frequently employed for this purpose is the introduction of time dependent collective coordinates. They reduce the full field equations to (coupled) ordinary differential equations. Though being an approximation relying on good guesses for appropriate collective coordinates, it assists to identify the relevant modes in case agreement between the solutions of the full and the reduced equations is obtained. Collective coordinates for the φ^4 model were suggested in Ref. [22] already some time ago. Numerical calculations were only performed later on [7,23,24] and yielded remarkable agreement with the solutions to the full field equations, thereby stressing the relevance of the shape mode for resonance formation. Unfortunately, a typographical error in a formula from Ref. [22] propagated into those numerical

---

[1]See Ref. [21] for an early review.

085008-1

studies [25]. Hence a second look at those studies is inevitable. Also, those studies included a subset of collective coordinates that is only appropriate for certain initial conditions. In addition a comprehensive collective coordinate study in the ϕ^6 model is important to illuminate the origin of the resonance solutions within kink-antikink scattering. These issues will be the objectives of the present paper.

In Sec. II we introduce the models that we consider. The collective coordinates are defined in Sec. III. In Sec. IV we present our numerical results. We summarize with a short conclusion in Sec. V. An appendix details the calculation of coefficient functions in the collective coordinate approach.

II. MODELS

The models that we consider are defined in one space and one time dimensions. From the onset, we use dimensionless variables (corresponding to $m = \sqrt{2}$ and $\lambda = 2$ in Ref. [22]) so that the Lagrange densities are

$$\mathcal{L}_4 = \frac{1}{2}\partial_\mu\varphi\partial^\mu\varphi - \frac{1}{2}(\varphi^2 - 1)^2 \quad \text{and}$$

$$\mathcal{L}_6 = \frac{1}{2}\partial_\mu\phi\partial^\mu\phi - \frac{1}{2}\phi^2(\phi^2 - 1)^2. \tag{1}$$

The respective field equations are partial differential equations (PDE),

$$\ddot{\varphi} - \varphi'' = 2\varphi(1 - \varphi^2) \quad \text{and}$$

$$\ddot{\phi} - \phi'' = -\phi(3\phi^4 - 4\phi^2 + 1), \tag{2}$$

that are straightforwardly obtained from the respective Lagrangians. In the above, dots and primes denote time and coordinate derivatives, respectively. There are two vacuum solutions in the φ^4 model, $\varphi_0 = \pm 1$ but three in the ϕ^6 model, $\phi_0 = \pm 1$ and $\phi_0 = 0$. The PDE allow for static soliton solutions that connect different vacuum solutions at spatial infinity. In the φ^4 model these are the kink and antikink solutions,

$$\varphi_{K,\bar{K}}(x) = \pm\tanh(x), \tag{3}$$

that are related by spatial reflection $x \leftrightarrow -x$. In the ϕ^6 model the soliton configurations that solve the field equations and connect the vacuum at $\phi_0 = 0$ with the vacua $\phi_0 = +1$ are

$$\phi_{K,\bar{K}}(x) = [1 + \exp(\pm 2x)]^{-\frac{1}{2}}. \tag{4}$$

Again these solutions are related by spatial reflection. In addition, the overall sign of $\phi_{K,\bar{K}}$ may be changed so that there are four different static solutions in the ϕ^6 model. Time dependent solutions are straightforwardly

constructed by a Lorentz boost: $x \to \frac{x-vt}{\sqrt{1-v^2}}$, with constant velocity v.

There is an important difference between the two models that concerns the small amplitude fluctuations about the soliton solutions. While there are zero modes in both models that emerge because the static solutions break translational invariance spontaneously, the φ^4 model has an additional bound state solution, the so-called shape or breather mode [1]. Parametrizing the field $\varphi(x, t) = \tanh(x) + \eta(x, t)$ and linearizing the PDE in η, this shape mode solution is found to be[2]

$$\eta(x, t) = e^{-i\sqrt{3}t}\chi(x) \quad \text{with}$$

$$\chi(x) = \frac{\sinh(x)}{\cosh^2(x)}. \tag{5}$$

The static solutions serve as initial conditions to investigate the kink-antikink system as a raw model for particle-antiparticle interactions. Initially a kink and antikink are widely separated while moving towards each other. To be precise, in the φ^4 model the initial conditions read

$$\varphi(x, 0) = \varphi_{\bar{K}}\left(\frac{x}{\sqrt{1-v^2}} - X_0\right) + \varphi_K\left(\frac{x}{\sqrt{1-v^2}} + X_0\right) - 1,$$

$$\dot{\varphi}(x, 0) = \frac{v}{\sqrt{1-v^2}}\left[\varphi'_{\bar{K}}\left(\frac{x}{\sqrt{1-v^2}} - X_0\right)\right.$$

$$\left. - \varphi'_K\left(\frac{x}{\sqrt{1-v^2}} + X_0\right)\right], \tag{6}$$

where the primes denote the derivative with respect to the argument. Here X_0 is a measure for the initial separation and v is the relative kink and antikink velocity.

The situation is slightly more complicated in the ϕ^6 model because two different scenarios can be built up. First there is the kink-antikink configuration

$$\phi_{K\bar{K}}(x, 0) = \phi_{\bar{K}}\left(\frac{x}{\sqrt{1-v^2}} + X_0\right)$$

$$+ \phi_K\left(\frac{x}{\sqrt{1-v^2}} - X_0\right) - 1,$$

$$\dot{\phi}_{K\bar{K}}(x, 0) = \frac{-v}{\sqrt{1-v^2}}\left[\phi'_{\bar{K}}\left(\frac{x}{\sqrt{1-v^2}} + X_0\right)\right.$$

$$\left. - \phi'_K\left(\frac{x}{\sqrt{1-v^2}} - X_0\right)\right], \tag{7}$$

and second the antikink-kink scenario

---

[2]The threshold is at $\omega = 2$ for the dimensionless variables adopted here.

$$\phi_{\bar{K}K}(x,0) = \phi_{\bar{K}}\left(\frac{x}{\sqrt{1-v^2}} - X_0\right) + \phi_K\left(\frac{x}{\sqrt{1-v^2}} + X_0\right),$$

$$\dot{\phi}_{\bar{K}K}(x,0) = \frac{v}{\sqrt{1-v^2}}\left[\phi'_{\bar{K}}\left(\frac{x}{\sqrt{1-v^2}} - X_0\right)\right.$$
$$\left. - \phi'_K\left(\frac{x}{\sqrt{1-v^2}} + X_0\right)\right]. \tag{8}$$

Using the above initial conditions with large X_0, the numerical solutions of the PDE (2) have been extensively discussed in the literature, both for the φ^4 [7,18,23,24,26] and ϕ^6 [19] models. Especially in the φ^4 model the multifaceted structures that emerge as the relative velocity v is changed have been widely explored. We elaborate on these structures in Sec. IV. See also Ref. [25] for a comparative discussion for both models and a collection of further references.

III. COLLECTIVE COORDINATES

Time dependent collective coordinates have mainly been considered for the φ^4 model. Initially [22] they were introduced to simplify the PDE to ordinary differential equations (ODE). Later, see e.g., [24] and references therein; they were utilized to explain the multiple bounce solutions within the kink-antikink collision that were earlier observed in the solutions to the PDE. In this context the shape mode, Eq. (5), plays a decisive role. It has been conjectured that this mode is excited during the collision and that this excitation absorbs too much energy from the kink-antikink system to fully separate. Only when the shape mode releases this energy in phase with the dissociation of kink and antikink do they possess enough energy to depart to spatial infinity. Hence the amplitude of the shape mode and the kink-antikink separation are important characteristics of the system and thus motivate us to introduce corresponding collective coordinates via

$$\varphi_c(x,t) = \varphi_K(\xi_+) + \varphi_{\bar{K}}(\xi_-) - 1$$
$$+ \sqrt{\frac{3}{2}}[A(t)\chi(\xi_-) + B(t)\chi(\xi_+)] \quad \text{where}$$
$$\xi_\pm = \xi_\pm(x,t) = \frac{x}{\sqrt{1-v^2}} \pm X(t). \tag{9}$$

Obviously, $X(t)$ is the collective coordinate for the separation while $A(t)$ and $B(t)$ are the amplitudes of the shape modes in the background of the antikink and kink, respectively. This *Ansatz* is substituted into the Lagrange density and, by spatial integration, a Lagrange function for the collective coordinates is obtained. Generically it takes the form

$$L_4(A,\dot{A},B,\dot{B},X,\dot{X}) = a_1(X)\dot{X}^2 - a_2(X) + a_3(X)\dot{A}^2$$
$$- a_4(X)A^2 + a_5(X)A + \cdots$$
$$+ b_3(X)\dot{B}^2 - b_4(X)B^2 + b_5(X)B$$
$$+ \cdots - d_{10}(X)AB^3. \tag{10}$$

The ellipsis refer to terms that involve other powers and products of the amplitudes A and B as derived from the Lagrangian, Eq. (1). Unless otherwise noted, they are included in our calculation though omitted above for brevity only. The coefficient functions, $a_1(X),\ldots,d_{10}(X)$, are obtained as spatial integrals of the kink and/or antikink profile functions. For example (see also the Appendix),

$$a_1(X) = \frac{1}{2}\int_{-\infty}^{\infty} dx[\phi'_K(\xi_+) - \phi'_{\bar{K}}(\xi_-)]^2$$
$$= \frac{4}{3}\sqrt{1-v^2}\left[1 + \frac{6X\coth(2X) - 3}{\sinh^2(2X)}\right].$$

Here we refrain from further listing those integrals in detail since they are documented in the appendixes of Ref. [27]. As indicated analytic expressions (as functions of X) can be obtained using analytic function theory [18,22,28]. Since we anyhow intend to perform numerical simulations, the numerical representation suits us well. From the above Lagrange function a set of coupled second order ODE is derived that governs the time evolution of the collective coordinates. Schematically they are cast into the form

$$\begin{pmatrix} a_{11} & a_{12} & a_{13} \\ a_{21} & a_{22} & a_{23} \\ a_{31} & a_{32} & a_{33} \end{pmatrix}\begin{pmatrix} \ddot{X} \\ \ddot{A} \\ \ddot{B} \end{pmatrix} = \begin{pmatrix} f_1 \\ f_2 \\ f_3 \end{pmatrix}$$
$$\Leftrightarrow \begin{pmatrix} \ddot{X} \\ \ddot{A} \\ \ddot{B} \end{pmatrix} = \begin{pmatrix} a_{11} & a_{12} & a_{13} \\ a_{21} & a_{22} & a_{23} \\ a_{31} & a_{32} & a_{33} \end{pmatrix}^{-1}\begin{pmatrix} f_1 \\ f_2 \\ f_3 \end{pmatrix}. \tag{11}$$

The matrix elements a_{mn} and the right-hand sides f_n contain the coefficient functions $a_i(X)$ etc. as well as factors of the collective coordinates themselves. For example,

$$a_{11} = 2[a_1(X) + a_6(X)A + a_8(X)A^2 + b_6(X)B$$
$$+ b_8(X)B^2 + d_2(X)AB].$$

The remaining lengthy formulas are reported in detail in Ref. [27]. The ODE, Eq. (11), are to be solved for initial conditions resembling those for the PDE from Sec. II, i.e., $X(0) = X_0$ and $\dot{X}(0) = \frac{-v}{\sqrt{1-v^2}}$. The amplitudes of the

shape modes and their time derivatives all vanish initially.

The *Ansatz*, Eq. (9), was already proposed in Ref. [22]. However, numerical calculations have only been performed for reduced sets. For example, the reduced system with $A(t) \equiv 0$ and $B(t) \equiv 0$ was solved in Ref. [18], while the subsystem[3] $A(t) \equiv -B(t)$ was comprehensively investigated in Ref. [24]. The latter restriction suffers from the obvious problem that $\chi(\xi_-) \sim \chi(\xi_+)$ at zero separation $X(t) \sim 0$ so that the amplitude $A(t)$ turns ill defined. This is known as the null-vector problem [29]. This problem has been restated recently [30] in a different context but no rigorous soliton has been established so far. Furthermore, a typographical error in the formula for $a_5(X)$ from Ref. [22] has propagated through the literature making most of the numerical simulations obsolete. We give details in Sec. IV A. Hence a reanalysis of these numerical approaches is essential.

The situation is slightly different in the ϕ^6 model because there is no shape mode in the fluctuation spectrum. Similar to the φ^4 model, however, multiple bounce solutions have also been observed from the PDE for the kink-antikink interaction in the ϕ^6 model [19,25]. As mentioned, the excitation of the shape mode during the kink-antikink interaction has been conjectured to cause the multiple bounce solutions in the φ^4 model. As a working hypothesis it thus seems very suggestive to include this degree of freedom as a representative of vibrational excitations in the collective coordinate *Ansatz* also for the ϕ^6 model. We therefore write

$$\bar{\phi}_{\text{cc}}(x, t) = \phi_K(\xi_-) + \phi_{\bar{K}}(\xi_+) - 1$$
$$+ \sqrt{\frac{3}{2}}[A(t)\chi(\xi_-) + B(t)\chi(\xi_+)], \quad (12)$$

$$\phi_{\text{cc}}(x, t) = \phi_K(\xi_+) + \phi_{\bar{K}}(\xi_-)$$
$$+ \sqrt{\frac{3}{2}}[A(t)\chi(\xi_-) + B(t)\chi(\xi_+)], \quad (13)$$

for the kink-antikink and antikink-kink systems, respectively. Again Lagrange functions are computed for the two *Ansätze* and second order ODE are obtained for the collective coordinates[4] $X(t)$, $A(t)$ and $B(t)$. These equations are straightforwardly obtained but lengthy. The interested reader may extract them from Ref. [27]. In Refs. [31,32] the calculation with $A(t) \equiv 0$ and $B(t) \equiv 0$ was performed. If that indeed was a sensible approximation, we should find that our extended parametrization in

---

[3]For initial conditions that comply with this restriction it remains a solution at all times.

[4]Of course, we are treating three distinct models defined by Eqs. (9), (12) and (13). It is a matter of convenience that no distinguishing symbols for the collective coordinates are introduced.

Eqs. (12) and (13) always yields negligible amplitudes of the vibrational shape mode.

IV. NUMERICAL RESULTS

In this section we report the results from the numerical simulations of the differential equations discussed above. We solve the PDE equations, $\partial_t^2 \phi(x, t) = \partial_x^2 \phi(x, t) - V'(\phi(x, t))$, as an initial value problem with the right-hand side computed on a grid with typically 12001 equidistant points for $x \in [-2X_0, 2X_0]$. The second spatial derivatives are obtained from a five point formula that employs the actual position (coordinate argument on the left-hand side of the PDE) and its two neighbors to the left and right. The PDE is then propagated in time with the help of an adaptive step size control. The initial configurations are taken from Eqs. (6)–(8). Though time consuming when so many points are implemented, this is a standard technique. In contrast to earlier studies of the ODE for the collective coordinates we use the numerical representation for the coefficient functions, $a_1(X)$, etc. that depend on the separation parameter X. Hence we do not have available these coefficients for arbitrary values of X needed in the numerical simulation. We therefore compute these coefficients for a large amount of values $X \in [-1.2X_0, 1.2X_0]$ before attempting to solve the ODE. When integrating the ODE we then utilize a Laguerre interpolation to access the coefficients for the required X as the ODE is propagated in time by an adaptive step size algorithm. To monitor the accuracy of numerically integrating the differential equations we verify that the total energy as obtained from the respective model Lagrangian is indeed time independent.

We want to compare solutions for the full field equations (2) to the results from the collective coordinate approximation (11) with identical initial conditions. This amounts to comparing $X(t)$ to twice the distance between the kink and the antikink in the PDE calculation. We extract this from the expectation value

$$\langle x \rangle_t = \frac{\int_0^\infty dx\, x \epsilon(t, x)}{\int_0^\infty dx\, \epsilon(t, x)}, \quad (14)$$

where

$$\epsilon(t, x) = \frac{1}{2}[\ddot{\varphi} + \varphi'' + (\varphi^2 - 1)^2] \quad \text{or}$$
$$\epsilon(t, x) = \frac{1}{2}[\ddot{\phi} + \phi'' + (\phi^2 - 1)^2 \phi^2] \quad (15)$$

are the energy densities of the respective models. This procedure is based on the observation that the energy density $[\epsilon(t, -x) = \epsilon(t, x)$, when the initial field configuration is reflection symmetric] is characterized by two peaks that move in time. One peak signals the position of the kink on the negative half line, the other moves with the antikink on the positive half line. By restricting the
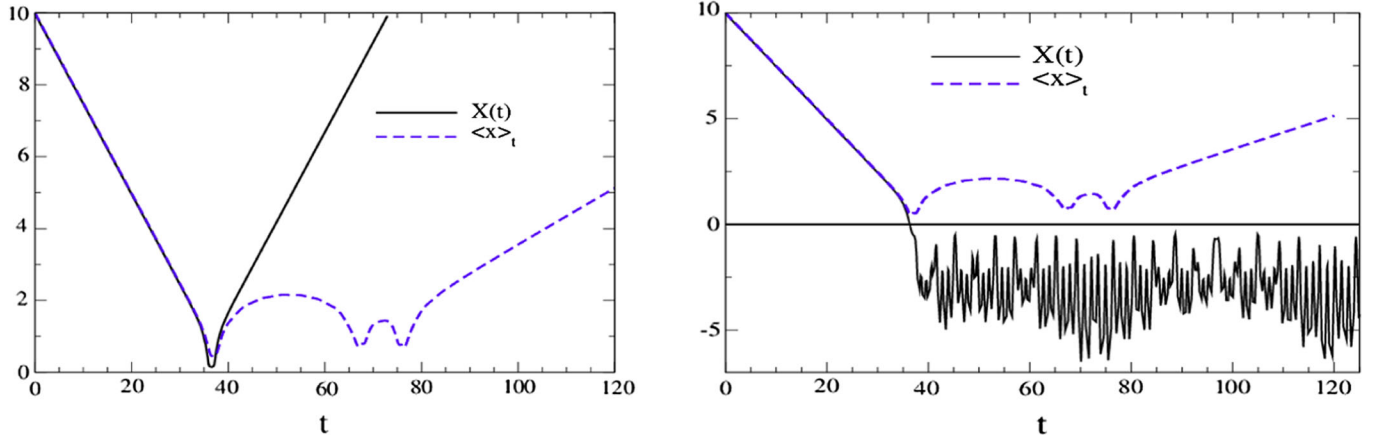
FIG. 1. Effect of correcting the linear coupling. The full lines show the time dependence of the collective coordinate $X(t)$ and the dashed lines picture the position of the antikink as extracted from the PDE according to Eq. (14). Left panel: calculation using $F(X)$ from Eq. (16); right panel: corrected coupling from Eq. (17). Either case has $v = 0.251$.

integration interval to $x \geq 0$ in Eq. (14), the position of the antikink is identified.

A. φ^4 model

In a first step we explore the consequences of correcting the source term for the amplitude of the shape mode, the coefficients $a_5(X)$ and $b_5(X)$, in the numerical simulation of the φ^4 model. Because of a typographical error in Ref. [22] the expression (here we list the formulas with $v = 0$, for simplicity)

$$F(X) = -3\pi\sqrt{\frac{3}{2}} \tanh^2(2X)[1 - \tanh^2(2X)] \quad (16)$$

that entered previous simulations must be corrected to

$$a_5(X) = -3\pi\sqrt{\frac{3}{2}}\left[2 - 2\tanh^3(X) - \frac{3}{\cosh^2(X)} + \frac{1}{\cosh^4(X)}\right]. \quad (17)$$

We derive this corrected equation in the Appendix. However, it is intuitively clear that Eq. (16) cannot be correct: the coefficient a_5 is the amplitude of the modification of a background configuration. If that configuration is a solution to the field equations, the coefficient must vanish. It is easy to see that for $x = 0$ the background $\varphi_K(X) - \varphi_{\bar{K}}(X) - 1 = 2\tanh(X) - 1$ is not a vacuum configuration when $X \to -\infty$. Hence $\lim_{X \to -\infty} a_5(X) \overset{!}{\neq} 0$. Obviously the expression in Eq. (16) violates this condition.[5] Note that reasonable approximations to the full

---

[5]Besides the convention regarding the arguments of the hyperbolic functions the essential typo from Ref. [22] is the power of the $\tanh(X)$ term in Eq. (17). If that is decreased to 2, the expression in square brackets indeed simplifies to $\tanh^2(X)[\tanh^2(X) - 1]$.

solutions were previously achieved by using $F(X)$ for the linear coupling [7,24]. Additional simplifications were assumed in those simulations: (i) direct couplings between the shape modes at $\pm X$ and (ii) interactions involving higher than quadratic powers of the shape were omitted. We reproduce the result of such a calculation in the left panel of Fig. 1. There is indeed a similarity to the exact solution from the PDE. Once the correction for the linear coupling is implemented this similarity is completely lost. For the particular case of $v = 0.251$ the kink-antikink system is trapped for an arbitrary long time during which it fluctuates around a negative value. In Ref. [25] similar fluctuations were reported for $v = 0.2$, where, however, the system separated after a long time.

The other approximations that were made previously are obviously possible explanations for this mismatch between the ODE and PDE results. Omitting the higher order couplings is also questionable in view of the results from Ref. [33]. A PDE calculation was performed for a wave packet moving towards a single φ^4 kink. Initially the wave packet and the kink were well separated and after the interaction the phase shift was extracted from the wave packet. Agreement with the phase shift from the harmonic approximation required the amplitude of the fluctuations about it not to exceed 0.01, which is a small value in the present context. (This does not invalidate formal results based on the harmonic approximation, like quantum corrections to kink properties that originate from the semiclassical $\hbar$ expansion.) So it is suggestive to omit such approximations in the next step. However, then we face the problem that the matrix in Eq. (11) may become singular. Indeed this is the case. As illuminated in the Appendix, symmetry relations among the coefficient functions like, for example, $a_5(X) = -b_5(X)$, unfold that $A(t) = -B(t)$ is a possible solution to the ODE. Hence, configurations that initially obey this relation do so for all t. But then $A(t)$ and $B(t)$ are ill defined when $X(t) = 0$. This
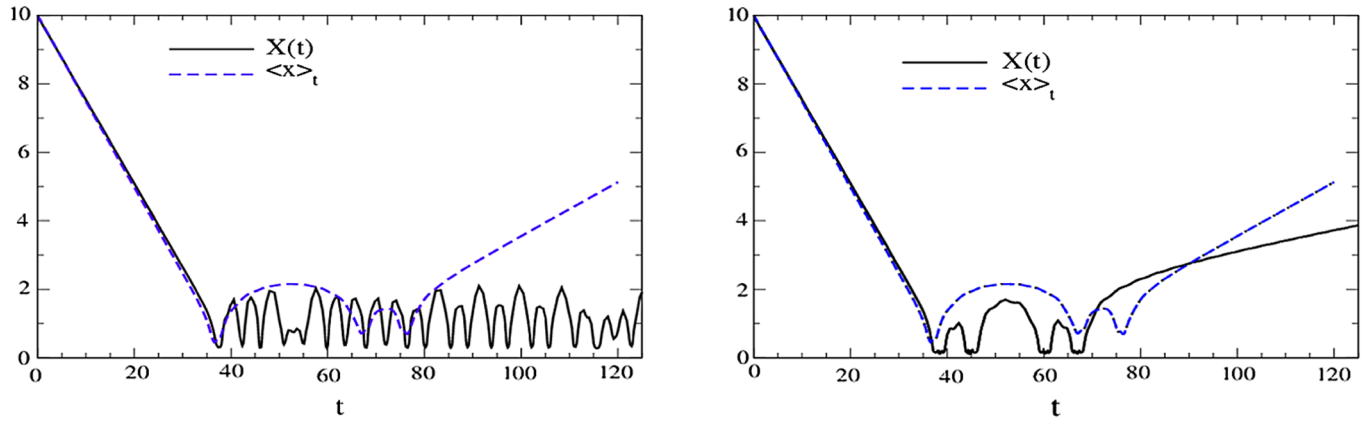
FIG. 2.   Solutions to the ODE with $v = 0.251$ and two different values $q = 5$ (left panel) and $q = 10$ (right panel) for the new parameter in Eq. (18).

is the null-vector problem that causes the matrix from Eq. (11) to be singular. Of course, no such singularity is seen in the PDE. Furthermore in the PDE there is no (obvious) obstacle that prevents the kink and antikink from penetrating. However, the collective coordinate parametrization is a not a solution to field equations for $X \to -\infty$ and $A(t) = B(t) = 0$. These mismatches can be circumvented by a small modification of the collective coordinate parametrization. For the φ^4 model

$$\varphi_c(x, t) = \varphi_K(\xi_+) + \varphi_{\bar{K}}(\xi_-) - \tanh(qX)$$
$$+ \sqrt{\frac{3}{2}}[A(t)\chi(\xi_-) + B(t)\chi(\xi_+)] \qquad (18)$$

is a possibility that introduces the new parameter $q > 0$. This is an attempt to improve the collective coordinate *Ansatz* and establish better agreement with the PDE results. Eventually it can also bypass the null-vector problem. Results for this parametrization are shown in Fig. 2. Obviously we observe only $X > 0$ and see that the PDE results are better approximated as q increases. Even though

$q > 0$ was introduced to allow $X \to -\infty$ its introduction has the opposite effect. A large q, which corresponds to not modifying the parametrization as long as $X > 0$, is needed to resemble the PDE results. This, however, induces large derivatives when $X \to 0^+$ that absorb energy and in turn prevent the configuration from assuming $X = 0$.

In Fig. 3 we compare the results for two different initial velocities of the ODE to the corresponding solutions of the PDE with particular emphasis on the amplitude of the shape mode. In each case the collective coordinate $X(t)$ has some qualitative similarity with the center of the energy density $\langle x \rangle_t$. More importantly we observe that the amplitude of the shape mode is strongly enhanced as the kink-antikink system shrinks. This suggests that indeed a significant amount of energy is stored in that mode during the collision. Once the kink and antikink have separated this amplitude is essentially 0.

B. ϕ^6 model

As in the φ^4 model the original collective coordinate parametrizations, Eqs. (12) and (13), describe vacuum
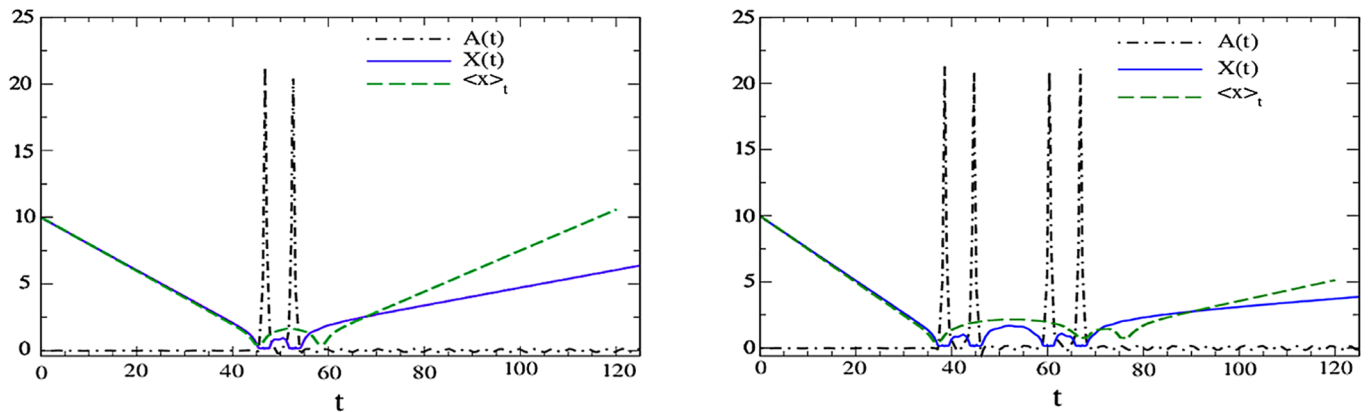

FIG. 3.   Effect of shape mode in the φ^4 model. ODE calculations with $q = 10$ in Eq. (18). Left panel: $v = 0.201$; right panel: $v = 0.251$.
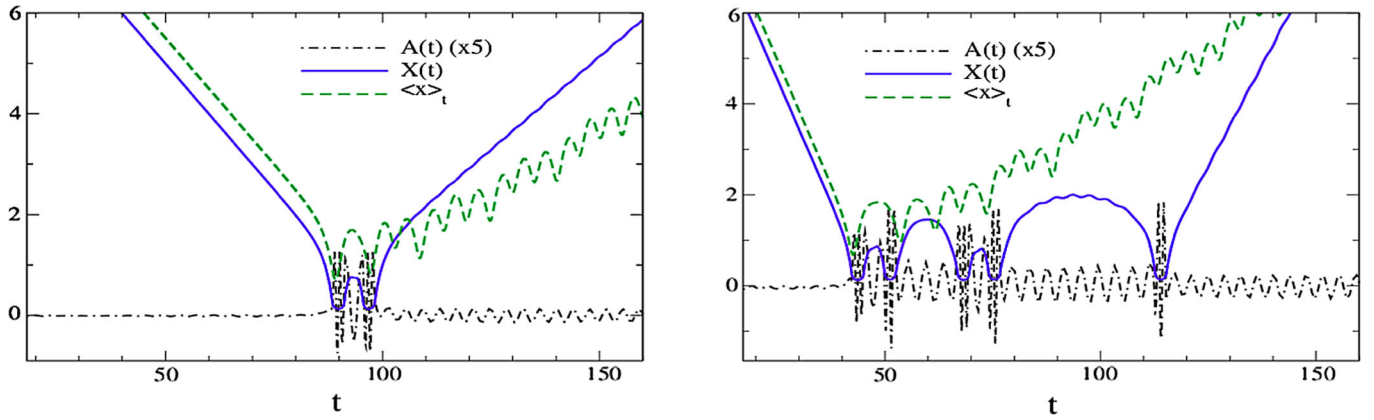
FIG. 4.   Effect of shape mode in the ϕ^6 model. ODE calculations with $q = 10$ in Eq. (19). Left panel: $v = 0.100$; right panel: $v = 0.221$.
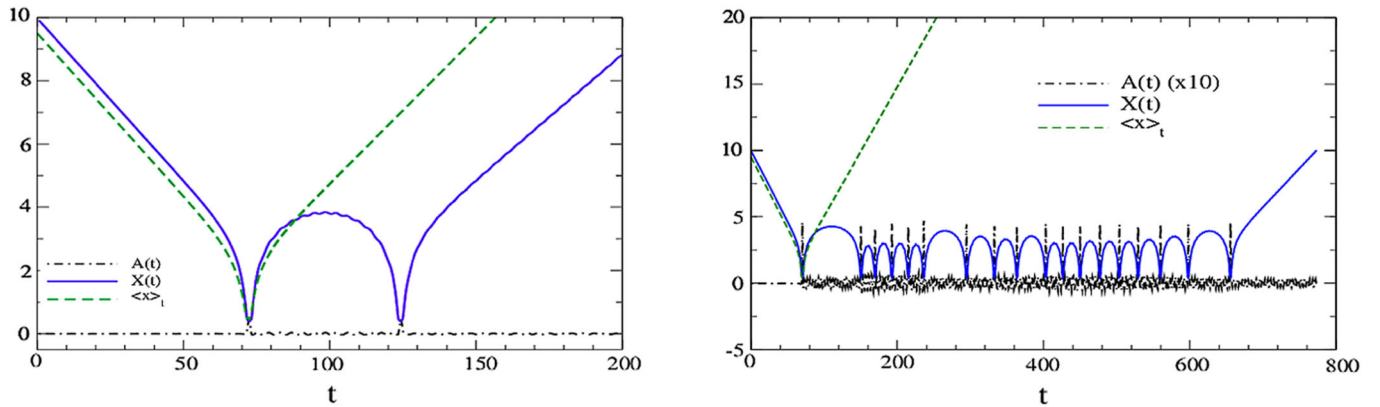

FIG. 5.   Effect of shape mode in the ϕ^6 model. ODE calculations with $q = 10$ in Eq. (20). Left panel: $v = 0.103$; right panel: $v = 0.111$.

configurations only for $X \ggg x$ but not for $X \lll x$. We therefore modify those parametrizations to

$$\bar{\phi}_{cc}(x, t) = \phi_K(\xi_-) + \phi_{\bar{K}}(\xi_+) - \frac{1}{2}[\tanh(qX) + 1]$$

$$+ \sqrt{\frac{3}{2}}[A(t)\chi(\xi_-) + B(t)\chi(\xi_+)], \qquad (19)$$

and

$$\phi_{cc}(x, t) = \phi_K(\xi_+) + \phi_{\bar{K}}(\xi_-) + \frac{3}{\sqrt{1 + e^{2qX}}}$$

$$+ \sqrt{\frac{3}{2}}[A(t)\chi(\xi_-) + B(t)\chi(\xi_+)]. \qquad (20)$$

We have adjusted the additional constant $q \approx 10$ from numerical experiments on the qualitative agreement with the PDE results.

In Fig. 4 we show the results for the kink-antikink interaction. We observe that the collective coordinate approximation reproduces the first resonance. However, at later times we observe significant deviations from the exact PDE results. In particular, the collective coordinate approximation does not reproduce the pronounced

oscillations on top of the kink-antikink pair drifting apart with constant velocity.

We show the results for the antikink-kink interaction arising from the initial condition of Eq. (20) in Fig. 5. In the two displayed cases the adopted initial velocity exceeds the critical velocity for bounces to occur in the PDE. In
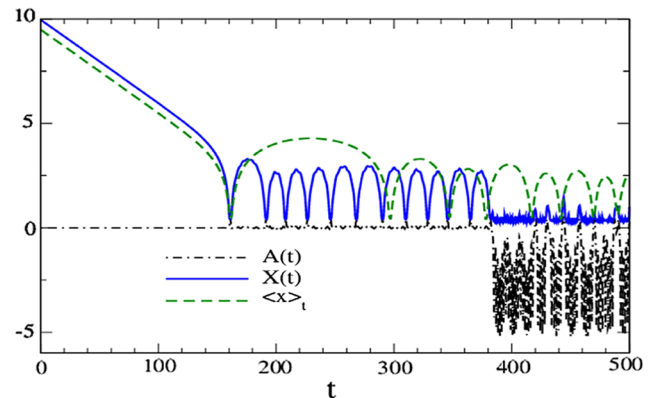

FIG. 6.   Effect of shape mode in the ϕ^6 model. ODE calculations with $q = 10$ in Eq. (20) for $v = 0.040$.

TABLE I.   Predictions for the critical velocities.

System	PDE	ODE
φ^4	0.26	0.4245
ϕ^6, $K\bar{K}$	0.289	0.4424
ϕ^6, $\bar{K}K$	0.0457	0.1119

contrast, the ODE produces bounces and for $v = 0.111$ there are many of them and the solution to the ODE is confined for a very long time.

As in the φ^4 model we see that indeed the shape mode gets excited as the kink and antikink get very close. However the corresponding amplitude $A(t)$ is not quite as pronounced in the ϕ^6 model. This suggests that other modes are also relevant for energy storage and resonance formation in the kink-antikink interaction of the ϕ^6 model.

In Fig. 6 we finally consider the scenario for the antikink-kink interaction where the PDE produces bounces. The collective coordinate approximation does so too, but the number of bounces differs in the two calculations. Even more interestingly, their results from the PDE and ODE calculations are similar for moderate times. But at even larger times the antikink-kink pair stays very close together with the energy dwelling in the amplitude of the shape mode within the ODE solution.

In Table I we list the predictions for the critical velocities above which resonances cease to exist. We recognize that the collective coordinate approximation reproduces the pattern but overestimates the exact results from the PDE.

V. CONCLUSION

We have revisited the collective coordinate approximations to the field equations of the φ^4 and ϕ^6 models in one time and one space dimensions. Various arguments have motivated this investigation. First, there has been an inconsistency in the literature about the source term of the vibrational mode (represented by the shape mode) in the φ^4 model. Second, in that model this vibrational excitation has previously been considered as the driving force for resonance solutions in the kink-antikink interaction. However, that mode is not part of the small amplitude spectrum in the ϕ^6 model which nevertheless contains resonance solutions. Third, identifying the amplitude of the shape modes for the kink and antikink leads to a singularity of the collective coordinate approximation when kink and antikink get arbitrarily close. To circumvent this so-called null-vector problem we have abandoned that identification. The structure of the equations of motion, however, revealed that this procedure does not fully resolve this singularity for initial conditions that parametrize a pure kink-antikink system at large separation. Additional modifications of the collective coordinate parametrization were necessary to achieve a nonsingular description. These modifications

were motivated by the search for a better approximation to the exact PDE solutions and introduced a novel parametrization of the fields in terms of the collective coordinates. With this new parametrization, the singular point was not part of the solution to the ODE and the null-vector problem did not occur. Fourth, many of the literature studies adopted the harmonic approximation for this amplitude (and other simplifications to avoid the null-vector problem). Since nonlinearity is an essential feature of these models, it was inevitable to go beyond this approximation.

We have seen that the collective coordinate approximations resemble the solutions to the full field equations only moderately well. Some of the resonances of the kink-antikink interactions are reproduced by solving the ODE of the collective coordinate approximations, but these solutions typically produce too many bounces. Also the ODE approach overestimates the relative initial velocities between the kink and antikink above which no bounces occur in all scenarios. On the other hand we have seen that the amplitudes of fluctuations (modeled by the shape mode) about the kink-antikink system are strongly enhanced during bounces, though it is significantly more pronounced in the φ^4 model than in the ϕ^6 model. This indeed suggests that energy is stored in these modes during the interaction. Unfortunately, the resemblance between the collective coordinate and the exact solutions is not good enough to turn that into the statement that the existence of a shape mode in the fluctuation spectrum is causal for the occurrence of multiple bounce solutions in kink-antikink scattering. Previous calculations with the distance between kink and antikink as the only collective coordinate (e.g., Ref. [18] for φ^4 and Ref. [32] for ϕ^6 models, respectively) found acceptable agreement with the exact field equations. However, if that had been an appropriate approximation our generalization should not have yielded sizable amplitudes for the additional variables.

APPENDIX: DERIVATION OF EQ. (17)

In this appendix we outline the derivation of the corrected source term for the shape mode. There are linear coupling terms in the derivative term $\partial_\mu \varphi \partial^\mu \varphi$ and in the potential $V(\varphi) = \frac{1}{2}(\varphi^2 - 1)^2$. We use the equation of motion for $\varphi_{K,\bar{K}}$ and integrate by parts to write, with $V'(\phi) = 2\phi(\phi^2 - 1)$,

$$F(X) = \int_{-\infty}^{\infty} dx \{V'(\varphi_K(x+)) + V'(\varphi_{\bar{K}}(x-X)) - V'(\varphi_K(x+X) + \varphi_{\bar{K}}(x-X) - 1)\} \frac{\sinh(x+X)}{\cosh^2(x+X)}$$

$$= 2 \int_{-\infty}^{\infty} dx \{\tanh(x+X)[\tanh^2(x+X) - 1] - \tanh(x-X)[\tanh^2(x-X) - 1]$$

$$- (\tanh(x+X) - \tanh(x-X) - 1)[(\tanh(x+X) - \tanh(x-X) - 1)^2 - 1]\} \frac{\sinh(x+X)}{\cosh^2(x+X)}. \quad (A1)$$

The boost factor $1/\sqrt{1-v^2}$ is straightforwardly included by rescaling the integration variable. The interesting terms are those in which X appears with both signs. As an example we work out

$$I(X) = \int_{-\infty}^{\infty} dx \tanh^3(x-X) \frac{\sinh(x+X)}{\cosh^2(x+X)} \quad (A2)$$

in detail. As suggested in Ref. [18] we first define the Fourier integral

$$I_k(X) = \int_{-\infty}^{\infty} dx e^{ikx} \tanh^3(x-X) \frac{\sinh(x+X)}{\cosh^2(x+X)}$$

$$= \int_{-\infty}^{\infty} dz e^{ikz} \frac{\sinh^3(z-X)}{\cosh^3(z-X)} \frac{\sinh(z+X)}{\cosh^2(z+X)} \quad (A3)$$

and take the limit $I(X) = \lim_{k\to 0} I_k(X)$. This Fourier integral can be evaluated by analytic integration methods and noting that there are two set of poles,

(1) second order poles at $z = iy_n - X$

(2) third order poles at $z = iy_n + X$,

with $y_n = (2n+1)\frac{\pi}{2}$. We close the contour in the upper half plane so that $n = 0, 1, \ldots$ is relevant. To extract the residues for the first set of poles we write $z = iy_n - X + \epsilon$ and expand all functions under the integral to linear order in the small parameter ϵ,

$$\cosh(z+X) \sim i(-1)^n \epsilon$$

$$\cosh(z-X) \sim -i(-1)^n [s_2 - \epsilon c_2]$$

$$\sinh(z+X) \sim i(-1)^n$$

$$\sinh(z-X) \sim -i(-1)^n [c_2 - \epsilon s_2]$$

$$e^{ikz} \sim e^{-iXk} e^{-(2n+1)\pi k/2} [1 + ik\epsilon], \quad (A4)$$

where we have abbreviated $c_2 = \cosh(2X)$ and $s_2 = \sinh(2X)$. Then the integrand in Eq. (A3) expands as

$$e^{ikz} \frac{\sinh^3(z-X)}{\cosh^3(z-X)} \frac{\sinh(z+X)}{\cosh^2(z+X)}$$

$$= i(-1)^n e^{-iXk} e^{-(2n+1)\pi k/2} [1 + ik\epsilon] \frac{c_2^3 - 3\epsilon c_2^2 s_2}{s_2^3 - 3\epsilon s_2^2 c_2} \frac{1}{\epsilon^2}$$

$$+ \mathcal{O}(\epsilon^0). \quad (A5)$$

The relevant term involves $\frac{1}{\epsilon}$ and produces the residue

$$R_n^{(1)} = (-1)^n e^{-iXk} e^{-(2n+1)\pi k/2} \left[3i \frac{c_2^2}{s_2^4} - k \frac{c_2^3}{s_2^3}\right]. \quad (A6)$$

Summing the geometric series $\sum_{n=0}^{\infty} (-1)^n e^{-n\pi k} = (1 + e^{-\pi k})^{-1}$ yields

$$\sum_{n=0}^{\infty} R_n^{(1)} = \frac{e^{-iXk}}{2\cosh(\pi k/2)} \left[3i \frac{c_2^2}{s_2^4} - k \frac{c_2^3}{s_2^3}\right]$$

$$\to \frac{3i}{2} \frac{c_2^2}{s_2^4} \quad \text{as} \quad k \to 0. \quad (A7)$$

Since the geometric series resulted in an expression that is finite as $k \to 0$, the $\mathcal{O}(k)$ parts in the expansion did not contribute to the final result. We now turn to the residues of type (2) which are more cumbersome to evaluate because the singularity is third order. Hence we must expand all functions under the integral to one higher power when writing $z = iy_n + X + \epsilon$,

$$\cosh(z+X) \sim i(-1)^n \left[s_2 + \epsilon c_2 + \frac{1}{2}\epsilon^2 s_2\right]$$

$$\cosh(z-X) \sim -i(-1)^n \epsilon \left[1 + \frac{1}{6}\epsilon^2\right]$$

$$\sinh(z+X) \sim i(-1)^n \left[c_2 + \epsilon s_2 + \frac{1}{2}\epsilon^2 c_2\right]$$

$$\sinh(z-X) \sim -i(-1)^n \left[1 + \frac{1}{2}\epsilon^2\right]$$

$$e^{ikz} \sim e^{iXk} e^{-(2n+1)\pi k/2} \left[1 + ik\epsilon - \frac{1}{2}k^2\epsilon^2\right]. \quad (A8)$$

We recognize that the n dependence is the same as for the type (1) singularities so that it will be sufficient to only keep terms that do not vanish in the limit $k \to 0$ when expanding the function under the integral in Eq. (A3),

$$e^{ikz}\frac{\sinh^3(z-X)}{\cosh^3(z-X)}\frac{\sinh(z+X)}{\cosh^2(z+X)}$$
$$= -i(-1)^n e^{iXk}e^{-(2n+1)\pi k/2}$$
$$\times\left\{\frac{(1+\frac{\epsilon^2}{2})^3}{(1+\frac{\epsilon^2}{6})^3}\frac{c_2+\epsilon s_2+\frac{\epsilon^2}{2}c_2}{[s_2+\epsilon c_2+\frac{\epsilon^2}{2}s_2]^2}\frac{1}{\epsilon^3}+\mathcal{O}(k)\right\}+\mathcal{O}(\epsilon^0).$$
$$(A9)$$

We read off the residue from the term with $\frac{1}{\epsilon}$,

$$R_n^{(2)} = -i(-1)^n e^{iXk}e^{-(2n+1)\pi k/2}$$
$$\times\left\{\frac{1}{s_2^4}\left[-\frac{1}{2}c_2 s_2^2+3c_2^3-c_s s_2^2\right]+\mathcal{O}(k)\right\}$$
$$= -i(-1)^n e^{iXk}e^{-(2n+1)\pi k/2}\left\{\frac{3}{2}\frac{c_2}{s_s^4}[c_2^2+1]+\mathcal{O}(k)\right\}.$$
$$(A10)$$

We can now sum the residues and take the limit $k\to 0$,

$$\sum_{n=0}^{\infty}R_n^{(2)} = -i\frac{e^{-iXk}}{2\cosh(\pi k/2)}\left\{\frac{3}{2}\frac{c_2}{s_2^4}[c_2^2+1]+\mathcal{O}(k)\right\}$$
$$\to -\frac{3i}{4}\frac{c_2}{s_2^4}[c_2^2+1].\qquad (A11)$$

Finally we multiply the sum of Eqs. (A7) and (A11) by $2\pi i$ and obtain

$$I(X) = \frac{3\pi}{2}\frac{1}{s_2^4}[c_2^3+c_2-2c_2^2].\qquad (A12)$$

Using the addition theorems $s_2 = 2\sinh(a)\cosh(a)$ and $c_2 = 2\cosh^2(a)-1 = 2\sinh^2(a)+1$ gives a further simplification that we list below together with other relevant integrals that are obtained by the same techniques,

$$\int_{-\infty}^{\infty}dx\tanh^3(x-X)\frac{\sinh(x+X)}{\cosh^2(x+X)}=\frac{3\pi}{8}\frac{2\cosh^2 X-1}{\cosh^4 X}$$

$$\int_{-\infty}^{\infty}dx\tanh^2(x-X)\tanh(x+X)\frac{\sinh(x+X)}{\cosh^2(x+X)}=\frac{\pi}{8}\frac{4\cosh^4 X-4\cosh^2 X+3}{\cosh^4 X}$$

$$\int_{-\infty}^{\infty}dx\tanh(x-X)\tanh^2(x+X)\frac{\sinh(x+X)}{\cosh^2(x+X)}=\frac{\pi}{8}\frac{4\cosh^2 X-1}{\cosh^4 X}$$

$$\int_{-\infty}^{\infty}dx\tanh(x-X)\tanh(x+X)\frac{\sinh(x+X)}{\cosh^2(x+X)}=\frac{\pi}{4}\frac{\tanh X}{\cosh^2 X}[1-2\cosh^2 X]$$

$$\int_{-\infty}^{\infty}dx\tanh(x-X)^2\frac{\sinh(x+X)}{\cosh^2(x+X)}=-\frac{\pi}{2}\frac{\tanh X}{\cosh^2 X}$$

$$\int_{-\infty}^{\infty}dx\tanh(x-X)\frac{\sinh(x+X)}{\cosh^2(x+X)}=\frac{\pi}{2}\frac{1}{\cosh^2 X}.\qquad (A13)$$

We have verified these integrals by numerical simulation. Some of the integrals are even in X while others are odd. Hence

$$F(X) = -3\pi\left[2-2\tanh^3 X-3\frac{1}{\cosh^2 X}+\frac{1}{\cosh^4 X}\right]\quad (A14)$$

does not have a specified transformation property under $X\leftrightarrow -X$, in contrast to the erroneous literature formula quoted in Eq. (16). Terms under the integral in Eq. (A1) that only have $x+X$ as arguments of the hyperbolic functions were obtained from the above list by setting $X=0$. Multiplying with the normalization of the shape mode ($\sqrt{\frac{3}{2}}$) gives the coefficient a_5 provided in Eq. (17).

To compute the coefficient b_5 we need to replace

$$\frac{\sinh(x+X)}{\cosh^2(x+X)}\to\frac{\sinh(x-X)}{\cosh^2(x-X)}$$
$$= -\frac{\sinh(-x+X)}{\cosh^2(-x+X)}\qquad (A15)$$

in Eq. (A1). Then $b_5 = -a_5$ because the term in curly brackets is invariant under $x\to -x$. This is one example for a general property of the collective coordinate Lagrangians, Eq. (10) and its ϕ^6 pendant; they are invariant under $A\leftrightarrow -B$.

For completeness we also outline the result for a_1 listed in Sec. III. It is interesting because the limit $k\to 0$ works differently from the above. Since $\frac{d}{dx}\tanh(x)=1/\cosh^2(x)$ the separation dependent part of a_1 requires the $k\to 0$ limit of

$$\int_{-\infty}^{\infty} dz \frac{e^{ikz}}{\cosh^2(x-X)\cosh^2(x+X)}. \quad (A16)$$

The singularities along the lines $\mathrm{Re}(z) = \pm X$ are second order and it suffices to consider Eqs. (A4) and (A8) to linear order in ϵ. The residues are

$$e^{\pm iXk}e^{-(2n+1)\pi k/2}\frac{1}{s_2^2}\left[ik \mp 2\frac{c_2}{s_2}\right] \quad \text{for} \quad z = iy_n \pm X. \quad (A17)$$

Summing all contributions yields

$$\frac{1}{2\sinh(\pi k)}\left[2\frac{c_2}{s_2}(e^{-iXk}-e^{+iXk})+ik(e^{-iXk}+e^{+iXk})\right]$$
$$\to \frac{-i}{\pi s_2^2}\left(2X\frac{c_2}{s_2}-1\right) \quad \text{as} \quad k \to 0. \quad (A18)$$

This is the separation dependent part of a_1.

[1] R. Rajaraman, *Solitons and Instantons* (North-Holland, Amsterdam, 1982).
[2] A. T. Avelar, D. Bazeia, L. Losano, and R. Menezes, Eur. Phys. J. C **55**, 133 (2008).
[3] T. S. Mendona and H. P. de Oliveira, J. High Energy Phys. 06 (2015) 133.
[4] V. A. Gani, V. Lensky, and M. A. Lizunova, J. High Energy Phys. 08 (2015) 147.
[5] T. Vachaspati, *Kinks and Domain Walls: An Introduction to Classical and Quantum Solitons* (Cambridge University Press, Cambridge, 2010).
[6] A. Vilenkin and E. P. S. Shellard, *Cosmic Strings and other Topological Defects* (Cambridge University Press, Cambridge, 2000).
[7] P. Anninos, S. Oliveira, and R. A. Matzner, Phys. Rev. D **44**, 1147 (1991).
[8] B. Ivanov, A. Kichiziev, and Y. N. Mitsai, Sov. Phys. JETP **75**, 329 (1992).
[9] A. R. Bishop, J. A. Krumhansl, and S. E. Trullinger, Physica (Amsterdam) **1D**, 1 (1980).
[10] G. 't Hooft, Nucl. Phys. **B72**, 461 (1974).
[11] E. Witten, Nucl. Phys. **B160**, 57 (1979).
[12] H. Weigel, Lect. Notes Phys. **743**, 1 (2008).
[13] D. T. J. Feist, P. H. C. Lau, and N. S. Manton, Phys. Rev. D **87**, 085034 (2013).
[14] N. S. Manton and P. Sutcliffe, *Topological Solitons* (Cambridge University Press, Cambridge, 2007).
[15] N. R. Quintero, A. Sánchez, and F. G. Mertens, Phys. Rev. Lett. **84**, 871 (2000).
[16] O. F. Oxtoby and I. V. Barashenkov, Phys. Rev. E **80**, 026609 (2009).
[17] G. Fodor, P. Forgacs, P. Grandclement, and I. Racz, Phys. Rev. D **74**, 124003 (2006).
[18] D. K. Campbell, J. F. Schonfeld, and C. A. Wingate, Physica (Amsterdam) **9D**, 1 (1983).
[19] P. Dorey, K. Mersh, T. Romanczukiewicz, and Y. Shnir, Phys. Rev. Lett. **107**, 091602 (2011).
[20] A. M. Marjaneh, D. Saadatmand, K. Zhou, S. V. Dmitriev, and M. E. Zomorrodian, arXiv:1605.09767.
[21] Y. S. Kivshar and B. A. Malomed, Rev. Mod. Phys. **61**, 763 (1989).
[22] T. Sugiyama, Prog. Theor. Phys. **61**, 1550 (1979).
[23] T. I. Belova and A. E. Kudryavtsev, Physica (Amsterdam) **32D**, 18 (1988).
[24] R. H. Goodman and R. Haberman, SIAM J. Appl. Dyn. Syst. **4**, 1195 (2005).
[25] H. Weigel, J. Phys. Conf. Ser. **482**, 012045 (2014).
[26] A. E. Kudryavtsev, Pis'ma Zh. Eksp. Teor. Fiz. **22**, 178 (1975) [JETP Lett. **22**, 82 (1975)].
[27] I. Takyi, MSc. thesis, Stellenbosch University, 2015, http://scholar.sun.ac.za/handle/10019.1/97877.
[28] M. Moshir, Nucl. Phys. **B185**, 318 (1981).
[29] J. G. Caputo and N. Flytzanis, Phys. Rev. A **44**, 6219 (1991).
[30] R. H. Goodman, A. Rahman, M. J. Bellanich, and C. N. Morrison, Chaos **25**, 043109 (2015).
[31] S. W. Goatham, arXiv:1209.3055.
[32] V. A. Gani, A. E. Kudryavtsev, and M. A. Lizunova, Phys. Rev. D **89**, 125009 (2014).
[33] A. M. H. H. Abdelhady and H. Weigel, Int. J. Mod. Phys. A **26**, 3625 (2011).